Chapter 11
The Hind- and Midfoot Alignment Analyzed After a Medializing Calcaneal Osteotomy Using a 3D Weight Bearing CT

Introduction

A medializing calcaneal osteotomy (MCO) is a surgical procedure frequently performed to correct an adult acquired flat foot deformity (AAFD) [1–3]. This condition is characterized by a complex 3D deformity resulting in a loss of the medial longitudinal arch, valgus alignment of the hindfoot, and abduction of the midfoot [4–7]. The initial treatment in mild deformities is conservative (e.g., insoles), but, once progression of the deformity and impairment of functional activities occur, surgery is advised [8]. In case a stage II AAFD, according to Johnson and Strom classification (containing a posterior tibial tendon dysfunction), does not respond to conservative treatment, a MCO is one of the surgical options available depending on the deformity characteristics [9]. The main goal of the procedure is to correct hindfoot alignment (HA) [3]. However, HA is markedly different among patients with stage II AAFD, and thus understanding how a MCO influences hindfoot alignment is essential. Chan et al. [10] have demonstrated a highly positive correlation between the change in the hindfoot moment arm and the amount of millimeters translated during a MCO. Although these findings have improved clinical practices, these measurements are still only performed on 2D radiographs and thus can be improved upon. Because 2D radiographs are a projection of a 3D deformity correction, 2D radiographs are prone to rotational errors and manual measurements. Laquinto et al. [11] addressed the limitations of 2D imaging but only for a 3D-simulated MCO model. Expanding upon this concept, Kido et al. [12] and subsequently Zhang et al. [13] utilized a 3D model in a clinical setting on patients with stage II AFFD. However, surgical corrections could not be assessed, and a CT scan was used to simulate weight bearing; the latter limitation can now be overcome by the use of a weight-

Based on Burssens A, Barg A, van Ovost E, Van Oevelen A, Leenders T, Peiffer M, Bodera I, WBCT ISG, Audenaert E, Victor J. The Hind- and Midfoot Alignment Computed after a Medializing Calcaneal Osteotomy using a 3D Weight bearing CT. *Int J Comp Assisted Radiol Surg* 2019;14(8) 1439–47.

M. Richter et al., *Weight Bearing Cone Beam Computed Tomography (WBCT) in the Foot and Ankle*, https://doi.org/10.1007/978-3-030-31949-6_11

bearing cone beam CT (WBCT) in foot and ankle pathologies [14]. This novel device allows for standing position images at a high resolution and at a relatively low radiation dose [14–17]. The application of a WBCT combined with currently available computed measurement techniques would overcome the aforementioned shortcomings and be for the first time applied in assessing a surgical hindfoot correction in 3D.

Our aim is to analyze the pre- and postoperative hind- and midfoot alignment after a MCO using a WBCT and 3D computed measurement techniques. We hypothesize that there is a linear relationship between the amount of medial translation during a MCO and the correction of both the hind- and midfoot alignment.

Material and Methods

Study Population, Design, and Measurement Protocol

Eighteen consecutive patients with mean age 41.8 years (SD = 17.3, range 19–62 years) were prospectively included between 2015 and 2017 after sustaining a medializing calcaneal osteotomy (MCO) and concomitant inframalleolar procedures (Table 11.1). Surgery was indicated for an adult acquired flat foot stage II ($N = 16$) or posttraumatic valgus deformity ($N = 2$). Exclusion criteria consisted of a tarsal coalition, age younger than 18 years or older than 65 years and concomitant supramalleolar procedures.

A prospective pre-post study design was used: pre- and postoperative weight bearing CT scans were collected before surgery and 12 weeks after surgery. The local Institutional Review Board approved the study (EC15/49/537), and all patients gave informed consent.

A PedCAT® weight bearing cone beam CT was used (CurveBeam, Warrington, PA, USA) containing the following imaging protocol and settings: tube voltage, 96 kV; tube current, 7.5 mAs; CTDIvol 4.3, mGy; matrix, 160,160,130; pixel size, 0.4 mm; and slice interval, 0.4 mm. At the department of radiology, patients were asked to assume a natural stance with both feet parallel to each other at shoulder width apart.

Table 11.1 Patient demographics and concomitant procedures

Characteristic	Total
Age (±) SD	41.8. ± 17.3 years
Sex (M/F)	4/14
TMT 1 fusion	2
Cotton osteotomy	4
Evans osteotomy	1
Gastroc release	11
FDL transfer	9
Spring ligament repair	3
Deltoid ligament reefing	1

In order to perform a 3D analysis, it is required to segment the CT slices based on their outer cortical surfaces. This was applied semiautomatic using the automatic bone segmentation tool in Mimics® 20.0 software (Materialise, Haasrode, Belgium) by manually appointing the cortical contour before Standard Triangulation Language (STL) files could be acquired. These were exported in 3-matic® software (Materialise, Haasrode, Belgium) to compute 3D goniometrical relationships.

A Cartesian coordinate system was acquired: the centroid of the talus was defined as the origin after being projected on the segmented base plate of the WBCT, to represent the ground floor [18]. The *z*-axis was defined as running through the origin and perpendicular to the segmented base plate. The *x*-axis runs through the origin and the projected centroid of the head of the second metatarsal, which simulates the longitudinal axis of the foot. The *Y*-axis was defined as the cross product of the *x*- and *z*-axis. The coronal plane was defined as the *YZ*-plane, the sagittal plane as the *XZ*-plane, and the axial plane as the *XY*-plane (Fig 11.4a–c).

This coordinate system was incorporated in a custom build script, using Matlab® 2016b (The MathWorks, Inc., MA, USA), and aligned pre- and postoperatively, in order to reference the computed angles and distances.

In general, each 3D measurement was determined pre- as well as postoperatively and subsequently projected in the reference plane currently used in clinical practice, to allow comparison and to optimize interpretation of the results.

The landmarks and axes necessary to calculate the following parameters were automatically computed by using the three main functions called "Create point: center of gravity," "Extrema analysis," and "Create line: fit inertia axis" function of the 3-matic® software. These are based on goniometric functions to calculate respectively the centroid of a generated volume, the most outer point of a structure in the direction of a given axis and best fit centroidal axis on a 3D model.

The hindfoot angle (HA) was determined in 3D by the intersection of the anatomical tibia axis (TA_x) and the talocalcaneal axis (TC_x) (Fig. 11.1a), as described previously [19]. The TA_x was computed as the best fitted longitudinal axis of the tibia shaft, manually marked above the incisura fibularis (Fig. 11.1b). Positive values equaled a valgus and negative values a varus hindfoot alignment. The TC_x was obtained after connecting computed centroid of the talus with the computed most inferior point of the calcaneus defined by Saltzman et al. [20] (Fig. 11.1d). Additionally, the TA_x and TC_x were measured separately towards the vertical axis in order to detect spatial changes as a consequence of the MCO.

The rotation of the tibia (TR) was determined by creating an axis (TR_x) connecting the computed most medial point of both the anterior and posterior tubercle using a build in goniometrical software function called (extrema analysis) (Fig. 11.1c, Supplementary Fig. 11.2a, b).

The difference in the axial plane between the pre- and postoperative (TR_x) allowed to determine the rotation of the tibia. Positive values equaled an external rotation and negative values an internal tibia rotation. The translations of the MCO were determined by reconstruction of the osteotomy plane (Fig. 11.2a). This allowed to divide the calcaneus in an anterior and posterior part (Fig. 11.2b). Based on the anterior part, the pre- and postoperative calcaneus could be matched on top of each

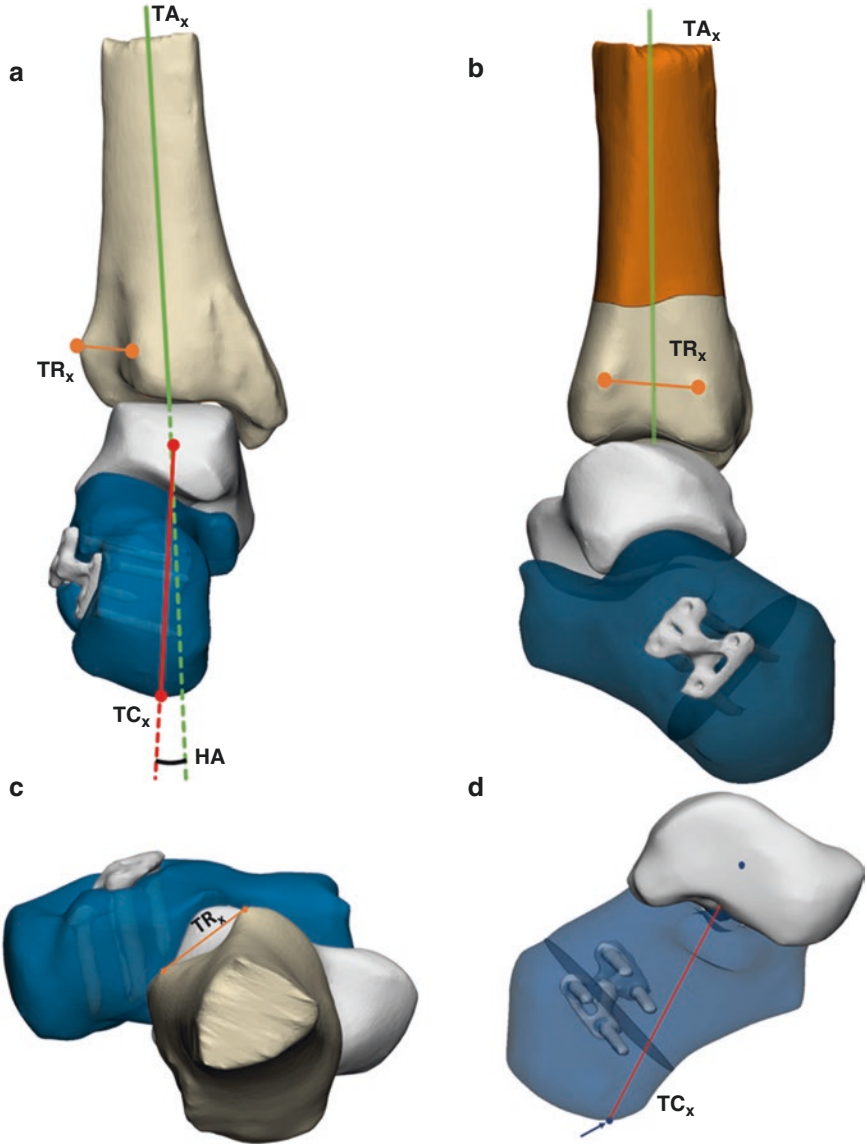

Fig. 11.1 Computed analysis of the hindfoot alignment (HA). (**a**) The (HA) was determined by the intersection of the anatomical tibia axis (TA_x) and the talocalcaneal axis (TC_x). (**b**) The TA_x was computed as the best fitted longitudinal axis above the incisura fibularis of the tibia shaft. (**c**) The TR_x was determined by connecting the computed most medial point of both the anterior and posterior tubercle of the incisura fibularis. (**d**) The TC_x was obtained after connecting the computed most inferior point of the calcaneus with the computed centroid of the talus

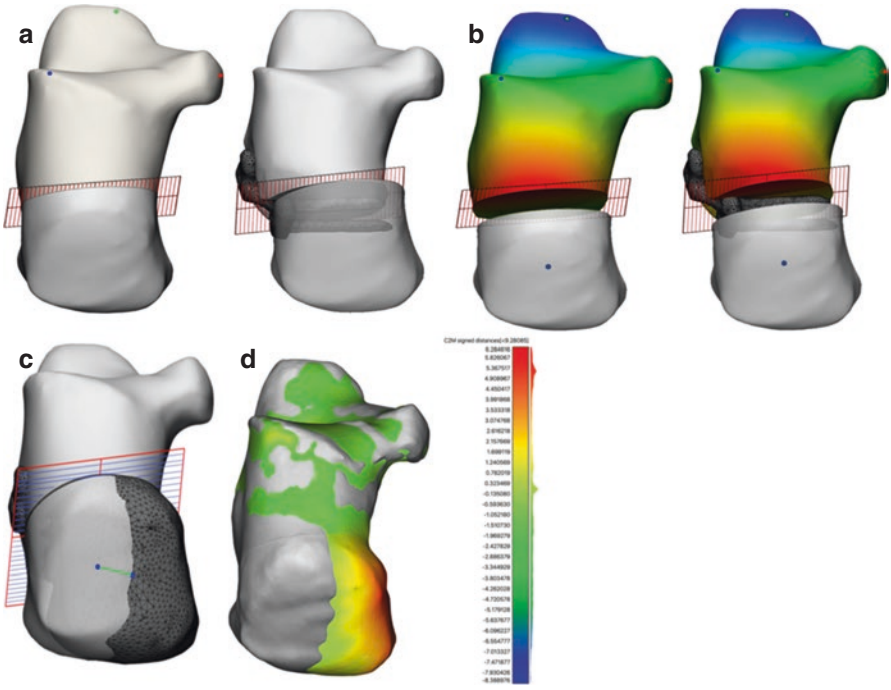

Fig. 11.2 Computing medial translation after a calcaneus osteotomy. (**a**) The osteotomy plane was reconstructed from the postoperative calcaneus. (**b**) Division of the calcaneus into an anterior and posterior part. The centroid of both posterior parts was computed. The anterior parts both preoperative (left) as well as postoperative (right) were fitted on top of each other. (**c**) The computed distance between the centroid of the pre- and postoperative posterior part of the calcaneus allowed for determination of the medial translation of the calcaneus osteotomy. (**d**) A deviation analysis depicting the range of the medial translation

other. The 3D distance between the computed centroid of the pre- and postoperative part of the posterior calcaneus was used to resemble the translation obtained after the MCO (Fig. 11.2c).

An additional deviation analysis was performed using CloudCompare® v 2.0 open source software (CloudCompare, Paris, France) by selecting the preoperative 3D model as a "mesh." This was automatically used as the reference and the postoperative model as a "cloud." The latter represented all vertices that form the 3D postoperative model. The distance between these vertices and the reference was determined by the CloudCompare®-software, and this analysis depicted the range of medial translation obtained after a MCO (Fig. 11.2d).

Measurements in the midfoot consisted of the navicular height (NH), navicular rotation (NR), and Méary angle (MA) [21].

The NH was determined as the distance between the computed most inferior point of the navicular and the ground (defined by the baseplate of the WBCT) (Fig. 11.3a). The NR was obtained by creating an axis (NR_x) going from the

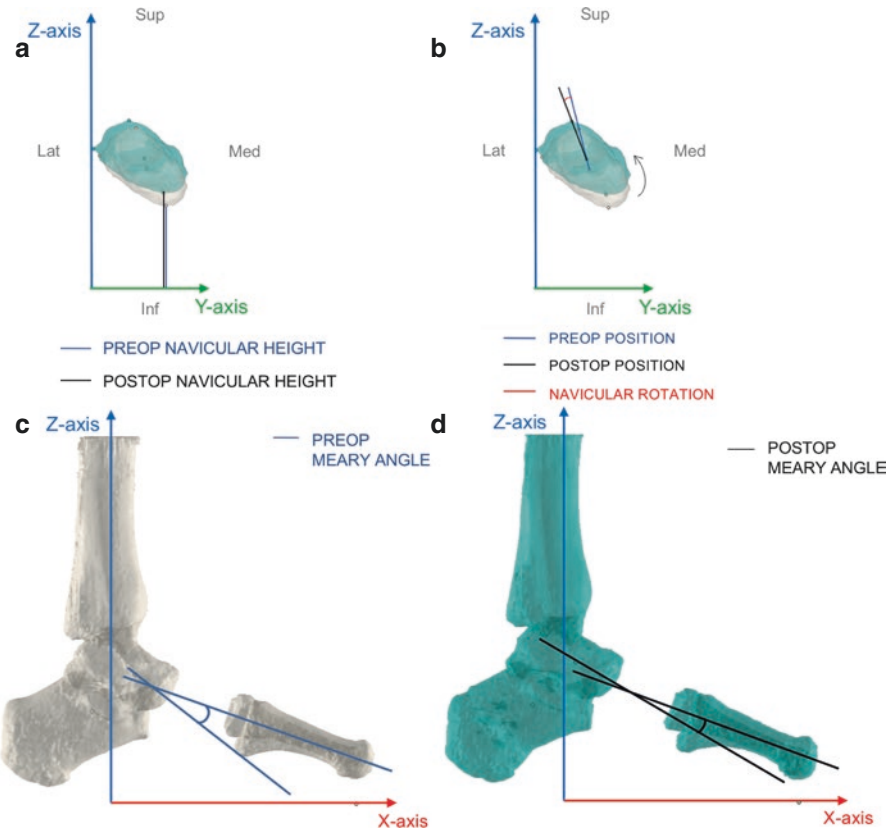

Fig. 11.3 Computed analysis of the midfoot alignment. (**a**) The navicular height (NH) was determined as the distance between the computed most inferior point of the navicular and the base plate (right); (**b**) the navicular rotation (NR) was obtained by creating an axis (NR_x) going from the computed most superior to inferior point of the navicular. The difference in the coronal plane between the pre- and postoperative NR_x helped determine the rotation of the navicular. (**c**) The Méary angle was determined preoperatively as the intersection of the best fitted longitudinal axis from the talar neck TN_x and the metatarsal axis MT_{1x}. (**d**) The same method was applied on the postoperative correction

computed most superior point of the navicular to the centroid of the navicular. The difference in the coronal plane between the pre- and postoperative NR_x allowed to determine the rotation of the navicular (Fig. 11.3b). Positive values equaled an inversion and negative values an eversion of the navicular. The Méary angle (MA) was determined in 3D by the intersection of the talus neck axis (TN_x) and the first metatarsal axis (MT_{1x}). Both axes were defined as a best fit centroidal axis respectively along the manually marked talar neck and computed selection of the first metatarsal (Fig. 11.3c–d). Positive values equaled a planus and negative values a cavus of the MA.

Surgical Procedure

The calcaneus was exposed through a lateral approach. The osteotomy was initiated with an oscillating saw blade 90° to the lateral calcaneal wall and inclined 45° in the sagittal plane according to Myerson et al. [1]. A broad osteotome was used to complete the medial cortex. The amount of medial translation of the calcaneum was determined by the surgeon (TL), based on intraoperative assessment with a neutral heel according to the longitudinal tibia axis. No additional rotation of impaction was performed. The osteotomy was fixated with either a 5 mm, 7.5 mm, or 10 mm calcaneus Step Plate® (Arthrex, Naples, FS, USA) with locking screws or was fixated by the use of two 7 mm cannulated lag screws (Wright Medical, Memphis, TN, USA). Postoperatively, patients were treated consistently with 6–8 weeks of non-weight bearing in a removable boot. This was followed by progression to full weight bearing between weeks 8 and 10, depending on healing.

Statistical Analysis

A Kolmogorov-Smirnov normal distribution test was performed for the hindfoot angle, rotation of the tibia, navicular height and rotation, and Méary angle. These demonstrated to be $P > 0.05$, indicating a normal distribution of the data and the use of further parametric testing. A paired Student's t-test was conducted to compare the means of the preoperative versus the postoperative measurements of both the hindfoot (HA, TAx, TCx, and TRx) and midfoot alignment (NH, NR, and MA).

The correlation between the measured hindfoot/midfoot alignment and amount of medial translation after MCO was assessed by the Pearson coefficient (R). Linear regression analysis was demonstrated by the use of a corresponding scatter plot and calculation of the R^2, when significant.

Inter- and intraobserver variability of the obtained midfoot measurements were analyzed using the interclass correlation coefficient [22]; the reliability of the hindfoot measurements was reported previously to be excellent [19].

Interpretations were as follows: ICC < 0.4, poor; 0.4 < ICC < 0.59, acceptable; 0.6 < ICC < 0.74, good; and ICC > 0.74, excellent [23].

The SPSS (release 22.0.0. standard version, SPSS, Inc., Chicago, IL, USA) statistical package was used to analyze the results. A probability level of $p < 0.05$ was considered significant.

An a priori statistical power analysis was performed using G∗Power (version 3.1.9.2; Dusseldorf University, Dusseldorf, Germany) [24]. Previously reported data regarding regression analysis of the hind- and midfoot alignment were used for sample size estimation [10]. Calculations have shown that a total sample size of $N = 4$ is needed for regression analysis of the hindfoot alignment and $N = 47$ for the midfoot alignment, to reach the respectively calculated effect size of ($f = 0.96$) and ($f = 0.33$) with a power level of 0.80 and a level of significance set at 0.05.

Results

Hindfoot Alignment

Pre- and Postoperative Comparison

A statistically significant difference was obtained in the HA3D, TAX 3D ($p < 0.001$), and TR3D ($p < 0.05$), when comparing pre- towards postoperative hindfoot measurements (Table. 11.2).

The intra- and interclass correlation coefficients were excellent both pre- and postoperatively (Table 11.4). The mean 3D translation obtained by the calcaneal osteotomy during surgery was 8.3 mm (SD = 4.2).

Regression Analysis

The Pearson coefficient showed a significant ($R = 0.926$, $p < 0.001$) correlation between the amount of medial calcaneal translation and the calculated change in HA3D angle. Linear regression analysis demonstrated a significant relationship ($R^2 = 0.84$, $p < 0.001$). The estimated change in hindfoot angle was expected to increase with 2.15° for every mm of MCO performed. The hindfoot angle could be predicted from the amount of MCO by the following equation (Fig. 11.4d): Change in hindfoot angle (degrees) = 2.15 (degrees/mm)· Amount of MCO (mm) − 3.39 3.2

Midfoot Alignment

Pre- and Postoperative Comparison

A statistically significant difference was obtained in the NH3D, NR3D ($p < 0.001$), and TR3D ($p < 0.05$), when comparing pre- towards postoperative midfoot measurements (Table. 11.3).

The intra- and interclass correlation coefficients were excellent both pre- and postoperatively (Table. 11.4).

Table 11.2 Comparison of pre- and postoperative hindfoot measurements

Hindfoot	Direction[a] preoperative			Postoperative		Change		
parameter	Measurement	Mean	SD	Mean	SD	Mean	95% CI	*p*-value
HA	Valg+/Var−	18.2	6.6	9.3	6.1	8.9	[5.9, 11.8]	<0.001
TA_x	Valg+/Var−	6.8	3.3	5.3	2.7	1.5	[1.7, 3.5]	<0.001
TC_x	Valg+/Var−	11.4	6.4	5.3	6.5	6.1	[4.1, 8.0]	<0.001
TR_x	Valg+/Var−	27.1	4.7	28.8	5.8	1.6	[0.4, 2.9]	0.016

[a]+ and – denote the direction of the measurement, *valg* valgus, *var* varus

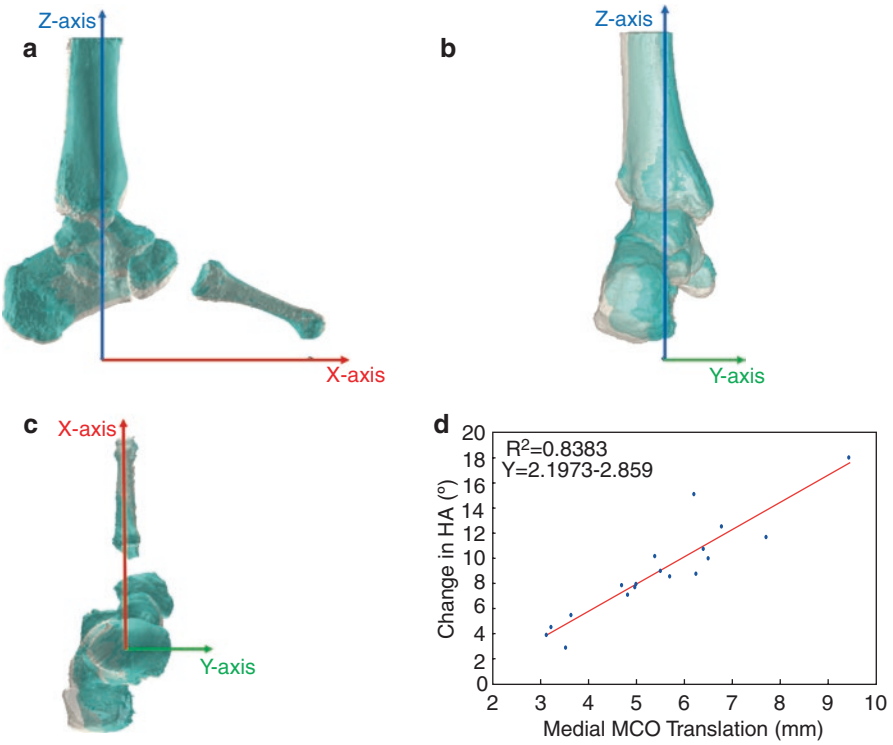

Fig. 11.4 Overview of the Cartesian coordinate system and linear regression analysis. (**a**) The centroid of the talus was defined as the origin after being projected onto the segmented base plate. (**b**) The *z*-axis was defined as running through the origin and perpendicular to the segmented base plate. (**c**) The *x*-axis runs through the origin and the projected centroid of the head of the second metatarsal, simulating the longitudinal axis of the foot. The *Y*-axis was defined as the cross product of the *x*- and *z*-axis. The coronal plane was defined as the *YZ*-plane, the sagittal plane as the *XZ*-plane, and the axial plane as the *XY*-plane. (**d**) Change in the hindfoot angle as a function of medical calcaneus translation. The obtained function can be used in clinical practice for preoperative planning

Table 11.3 Comparison of pre- and postoperative midfoot measurement

Midfoot	Direction[a] preoperative			Postoperative		Change		
parameter	Measurement	Mean	SD	Mean	SD	Mean	95% CI	*p*-value
NH	Prox+/Dist−	33.1	7.6	37.1	7.5	3.9	[2.5, 5.2]	<0.001
NR	Inv+/Ev−	16.3	5.1	22.7	6.5	6.4	[4.2, 8.4]	<0.001
MA	Plan+/Cav−	20.2	7.8	15.0	9.3	5.8	[8.4, 2.0]	<0.05

[a]+ and – denote the direction of the measurement; prox, proximal; dist, distal; inv, inversion; ev, eversion; plan, planus; cav, cavus

Table 11.4 Midfoot intra- and interclass correlation coefficients

Midfoot	ICC			
parameter	Preoperative		Postoperative	
	Intra	Inter	Intra	Inter
NH	0.999	0.999	0.999	0.999
NR	0.999	0.975	0.991	0.949
MA	0.849	0.848	0.896	0.868

Regression Analysis

The Pearson coefficient showed a nonsignificant ($p < 0.05$) correlation between the amount of medial calcaneal translation and the calculated change in NH, NR, and Méary angle (RNH = 0.38, $p = 0.16$; RNR = 0.32, $p = 0.24$; RMéary = 0.02, $p = 0.94$).

Discussion

This study shows an effective correction of the hindfoot valgus in an AAFD after a MCO assessed by a 3D weight bearing CT. It appears that the correction is not only situated in the calcaneus but also to a lesser extent in the tibia, resulting in 10% of the achieved HA correction.

Additional changes in the midfoot alignment were detected after a MCO combined with concomitant procedures: these could point a significant radiographic improvement of the navicular height/rotation and Méary angle.

These novel findings can be attributed to the application of 3D weight bearing and computed assessment of both the hindfoot and the midfoot correction, overcoming the previously encountered superposition and manual measurement methods on 2D plane radiographs [25].

The proposed formula, based on the regression analysis of the hindfoot correction, can be used when performing a 3D preoperative planning of an AAFD, since most of the current planning is based on intraoperative assessment [1, 3].

The obtained findings parallel previous research from Chan et al. [10], demonstrating a higher linear relationship between the amount of medial translation during a calcaneal osteotomy and the hindfoot correction when compared to the midfoot. This was also pointed out in other clinical and computed studies assessing changes in the midfoot alignment, which tended to be less pronounced compared to the hindfoot alignment after an MCO [1, 11]. The detected rotation of the navicular was consistent with previous reports demonstrating a higher eversion of the navicular, ranging from 2.3° to 6.2°, when flat foot deformity was more pronounced [12, 13]. These studies applied a similar measurement method but demonstrated shortcomings using a simulated weight bearing CT, which were overcome by a weight bearing CT in the present study.

The obtained results question the generally accepted osteotomy rule of 1 mm translation causing 1° of correction in knee and foot deformities [26, 27]. This could be attributed towards the 3D measurements containing more spatial data but was previously already shown in other studies containing 2D measurements in deformity corrections [10, 28].

We acknowledge that our study has several important limitations. Firstly, the study group consists of a low case number and is heterogeneous. The sample size calculation demonstrated to be sufficient towards regression analysis of the hindfoot alignment, but not for the midfoot alignment. In addition, midfoot measurements should be interpreted with respect to the performed concomitant procedures such as a FDL transfer, cotton osteotomy, or TMT fusion. The relative contribution of each procedure is difficult to analyze due to the size of the cohort and variation in full activity of an FHL transfer [29]. However, the described computed method could measure postoperative changes in the midfoot alignment, which were not detectible using previous imaging techniques [10].

Two patients were included with a posttraumatic valgus deformity of the calcaneus, containing a different pathoanatomy compared to an AAFD stage II. Despite this difference, a medializing calcaneus osteotomy is indicated as one of the treatment options in these posttraumatic deformities, and data concerning the radiographic outcome are limited [30], advocating the use of the applied measurement method. Moreover, the current preoperative planning is based on the classification of Stephens which uses a non-weight bearing CT, possibly underestimating the deformity during stance [31].

Second, all patients received a medial translation of the calcaneus, although other displacements during the osteotomy were avoided and small rotational changes could not be ruled out. Thirdly, not all radiographic measurement parameters of an AAFD were obtained pre- and postoperatively, but the most relevant ones for clinical practice were used [21]. Finally, the obtained results could have been influenced by the absence of scales or devices used to assess quantitatively if the patient was bearing full weight during the scanning process. However, postoperative scans were obtained at 3 months after surgical corrections, in order to avoid limitations in full weight bearing caused by antalgic reasons.

In conclusion, this study proposes a clinically relevant 3D method to compare the preoperative with the postoperative hind- and midfoot alignment after a MCO. In addition, a formula is provided to determine the required amount of medial translation during a calcaneus osteotomy to obtain the desired hindfoot correction and to prevent an overcorrection.

Future research can be aimed at validating this formula in clinical practice using prospective studies in cohorts stratified according to the concomitant procedure accompanying the MCO. These should incorporate patient-reported outcome scores (PROMS) to assess which amount of hindfoot correction is most beneficial for the patient [32, 33]. Furthermore, technical improvements such as built-in pressure sensors would allow to quantify and standardize the amount of weight applied on the foot, as currently been used to perform pedography in a weight bearing CT [34].

Additional 3D measurements can be aimed at the orientation of the osteotomy to determine which plane is the most optimal biomechanically as was already assessed in 2D by Reilingh et al. [35]. These data could be implemented to develop patient-specific guides as well as protocols for a computer-assisted surgical correction [36, 37].

References

1. Myerson MS, Badekas A, Schon LC. Treatment of stage II posterior tibial tendon deficiency with flexor digitorum longus tendon transfer and calcaneal osteotomy. Foot Ankle Int. 2004;25(7):445–50.
2. Yontar NS, Ogut T, Guven MF, Botanlioglu H, Kaynak G, Can A. Surgical treatment results for flexible flatfoot in adolescents. Acta Orthop Traumatol Turc. 2016;50(6):655–9.
3. Zaw H, Calder JDF. Operative management options for symptomatic flexible adult acquired flatfoot deformity: a review. Knee Surg Sports Traumatol Arthrosc. 2010;18(2):135–42.
4. McCormack AP, Ching RP, Sangeorzan BJ. Biomechanics of procedures used in adult flatfoot deformity. Foot Ankle Clin. 2001;6(1):15–23.
5. Alley MC, Shakked R, Rosenbaum AJ. Adult-acquired flatfoot deformity. JBJS Rev. 5(8):e7–e72017;5(8):e7–e.
6. Haddad SL, Myerson MS, Younger A, Anderson RB, Davis WH, Manoli A. Adult acquired flatfoot deformity. Los Angeles: SAGE Publications Sage CA; 2011.
7. Blackman AJ, Blevins JJ, Sangeorzan BJ, Ledoux WR. Cadaveric flatfoot model: ligament attenuation and Achilles tendon overpull. J Orthop Res. 2009;27(12):1547–54.
8. Wade M, Li Y-C, Wahl GM. Effect of therapeutic insoles on the medial longitudinal arch in patients with flatfoot deformity: a three-dimensional loading computed tomography study. Clin Biomech. 2013;13(2):83–96.
9. Ling SK-K, Lui TH. Posterior tibial tendon dysfunction: an overview. Open Orthop J. 2017;11(Suppl-4, M12):714–23.
10. Chan JY, Williams BR, Nair P, Young E, Sofka C, Deland JT, et al. The contribution of medializing calcaneal osteotomy on hindfoot alignment in the reconstruction of the stage II adult acquired flatfoot deformity. Foot Ankle Int. 2013;34(2):159–66.
11. Iaquinto JM, Wayne JS. Effects of surgical correction for the treatment of adult acquired flatfoot deformity: a computational investigation. J Orthop Res. 2011;29(7):1047–54.
12. Kido M, Ikoma K, Imai K, Maki M, Takatori R, Tokunaga D, et al. Load response of the tarsal bones in patients with flatfoot deformity: in vivo 3D study. Foot Ankle Int. 2011;32(11):1017–22.
13. Zhang Y, Xu J, Wang X, Huang J, Zhang C, Chen L, et al. An in vivo study of hindfoot 3D kinetics in stage II posterior tibial tendon dysfunction (PTTD) flatfoot based on weight-bearing CT scan. Bone Joint Res. 2013;2(12):255–63.
14. Barg A, Bailey T, Richter M, Netto C, Lintz F, Burssens A, et al. Weightbearing computed tomography of the foot and ankle: emerging technology topical review. Foot Ankle Int. 2018;39(3):376–86.
15. Lintz F, Cesar Netto CD, Barg A, Burssens A, Richter M, Group WBCIS. Weight-bearing cone beam CT scans in the foot and ankle. EFORT Open Rev. 2018;3(5):278–86.
16. Roemer W, Dufour AB, Gensure RH, Hannan MT, Hannan T, Dufour AB, et al. Flatfeet are associated with knee pain and cartilage damage in older adults. Arthritis Care Res. 2012;63:7.
17. de Cesar Netto C, Schon LC, Thawait GK, da Fonseca LF, Chinanuvathana A, Zbijewski WB, et al. Flexible adult acquired flatfoot deformity: comparison between weight-bearing and non-weight-bearing measurements using cone-beam computed tomography. J Bone Joint Surg Am. 2017;99(18):e98.

18. Kuo C-C, Lu H-L, Lu T-W, Lin C-C, Leardini A, Kuo M-Y, et al. Effects of positioning on radiographic measurements of ankle morphology: a computerized tomography-based simulation study. Biomed Eng Online. 2013;12(1):131.
19. Burssens A, Peeters J, Peiffer M, Marien R, Lenaerts T, ISG W, et al. Reliability and correlation analysis of computed methods to convert conventional 2D radiological hindfoot measurements to a 3D setting using weightbearing CT. Int J Comput Assist Radiol Surg. 2018;13(12):1999–2008.
20. Saltzman CL, El-Khoury GY. The hindfoot alignment view. Foot Ankle Int. 1995;16(9):572–6.
21. Younger AS, Sawatzky B, Dryden P. Radiographic assessment of adult flatfoot. Foot Ankle Int. 2005;26(10):820–5.
22. Auricchio F, Marconi S. 3D printing: clinical applications in orthopaedics and traumatology. EFORT Open Rev. 2016;1(5):121–7.
23. Shrout PE, Fleiss JL. Intraclass correlations: uses in assessing rater reliability. Psychol Bull. 1979;86(2):420.
24. Faul F, Erdfelder E, Buchner A, Lang A-G. Statistical power analyses using G∗ power 3.1: tests for correlation and regression analyses. Behav Res Methods. 2009;41(4):1149–60.
25. Richter M, Seidl B, Zech S, Hahn S. PedCAT for 3D-imaging in standing position allows for more accurate bone position (angle) measurement than radiographs or CT. Foot Ankle Surg. 2014;20(3):201–7.
26. Baig M, Baig U, Tariq A, Din R. A prospective study of distal metatarsal chevron osteotomies with K-wire fixations to treat hallux valgus deformities. Cureus. 2017;9(9):e1704.
27. Todd M, Lalliss S, DeBerardino T. A simplified technique for high tibial osteotomy with early radiographic follow-up results. Tech Knee Surg. 2008;7(3):172–7.
28. Amis AA. Biomechanics of high tibial osteotomy. Knee Surg Sports Traumatol Arthrosc. 2013;21(1):197–205.
29. Spratley EM, Arnold JM, Owen JR, Glezos CD, Adelaar RS, Wayne JS. Plantar forces in flexor hallucis longus versus flexor digitorum longus transfer in adult acquired flatfoot deformity. Foot Ankle Int. 2013;34(9):1286–93.
30. Nickisch F, Anderson RB. Post–calcaneus fracture reconstruction. Foot Ankle Int. 2006;11(1):85–103.
31. Stephens HM, Sanders R. Calcaneal malunions: results of a prognostic computed tomography classification system. Foot Ankle Int. 1996;17(7):395–401.
32. Conti MS, Ellis SJ, Chan JY, Do HT, Deland JT. Optimal position of the heel following reconstruction of the stage II adult-acquired flatfoot deformity. Foot Ankle Int. 2015;36(8):919–27.
33. Cöster MC, Bremander A, Rosengren BE, Magnusson H, Carlsson Å, Karlsson MK. Validity, reliability, and responsiveness of the Self-reported Foot and Ankle Score (SEFAS) in forefoot, hindfoot, and ankle disorders. Acta Orthop. 2014;85(2):187–94.
34. Richter M, Lintz F, Zech S, Meissner SA. Combination of PedCAT weightbearing CT with pedography assessment of the relationship between anatomy-based foot center and force/pressure-based center of gravity. Foot Ankle Int. 2018;39(3):361–8.
35. Reilingh M, Tuijthof G, Van Dijk C, Blankevoort L. The influence of foot geometry on the calcaneal osteotomy angle based on two-dimensional static force analyses. Arch Orthop Trauma Surg. 2011;131(11):1491–7.
36. Ma B, Kunz M, Gammon B, Ellis RE, Pichora DR. A laboratory comparison of computer navigation and individualized guides for distal radius osteotomy. Int J Comput Assist Radiol Surg. 2014;9(4):713–24.
37. Wei M, Chen J, Guo Y, Sun H. The computer-aided parallel external fixator for complex lower limb deformity correction. Int J Comput Assist Radiol Surg. 2017;12(12):2107–17.